Hittite Journal of Science and Engineering, 2018, 5(3) 225-230
ISSN NUMBER: 2148-4171
DOI: 10.17350/HJSE19030000099

Preparation of Molecular Sentinel Based SERS Sensor for Hepatitis C Virus

Adem Zengin
Van Yuzuncu Yil University, Department of Chemical Engineering, Van, TURKEY

ABSTRACT

Construction of a rapid, cost-effective and label free biosensor is important issue for public health. In this study, it has been developed a sensitive, selective and simple biosensor for the detection of hepatitis C virus (HCV) DNA. For this purpose, firstly, superparamagnetic gold nanoparticles were prepared by simple citrate reduction method and used as surface enhanced Raman spectroscopy (SERS) substrate. Then, Raman labelled hairpin DNA (molecular sentinel, MS) was covalently bound on the gold shell by means of gold-sulfur interaction. After addition the complementary DNA (target HCV DNA), the hairpin structure was changed closed state (stem-loop configuration) to open state (hybridization configuration). As a result, the Raman label was located far away from the surface and reduced the SERS intensity. A good relationship was obtained between the decreasing of the SERS intensity and the target DNA concentration (0-50 pM) and the limit of detection was found to be 0.1 pM. The sensing method only consists of a single hybridization and washing procedure after hybridization and centrifuge step can be omitted. It is believed that the prepared biosensor could be a powerful diagnostic tool for HCV detection.

Keywords:
Magnetic gold nanoparticles, Molecular sentinel and surface enhanced Raman spectroscopy.

Article History:
Received: 2017/10/10
Accepted: 2017/12/03
Online: 2017/12/22

***Correspondence to**: Adem Zengin,*
Van Yuzuncu Yil University, Department of Chemical Engineering, Tuşba, Van, Turkey.
Tel: +90 (432) 225-1726
Fax:+90 (432) 225-1730
E-Mail: ademzengin@yyu.edu.tr

INTRODUCTION

Hepatitis C is among the smallest known viruses and can lead to severe consequences that can go as far as carcinoma and liver cancer [1]. Hepatitis C virus (HCV) is usually transmitted to human through blood and sexual intercourse. Hepatitis C can develop in two ways: acutely or chronically. Acute Hepatitis C is a short-term illness that lasts about 6 months after infection. However, in the majority of patients (75-85%) acute hepatitis C infection becomes chronic which is a life-long disease and can lead to serious health problems (cirrhosis, liver cancer) and even death [2]. Hepatitis C usually does not have symptoms and can therefore be fatal. So, it is very important to detect HCV in early stage of infection to prevent serious health problems. Nowadays, enzyme-linked immunosorbent assay (ELISA) is frequently used for HCV detection [3]. Despite highly selective and specific measurements are carried out with this method, there are serious disadvantages such as not being able to determine in the early stages of the disease and not getting the accurate results in human immunodeficiency (HIV) infected patients. Moreover, several conventional analytical methods were developed for detection of HCV such as electrochemical [4], chemiluminescence [5], piezoelectric sensor [6], etc. Most of the aforementioned methods are often time consuming, require large amount of solvent, complicated operation and expensive equipment although HCV can be detected at low concentrations by those methods.

Surface enhanced Raman spectroscopy (SERS) is a type of Raman spectroscopy which generates enhanced Raman scattering from an analyte molecule that was adsorbed on metal surfaces. The scattering intensity increases depending on the analyte type, analyte position on metal surface, distance between analyte and metal surface and metal type [7]. Thanks to the careful selection of metal and analyte molecules, the SERS mechanism allows the determination of the analyte molecule at considerably lower concentrations as compared with other spectroscopic methods. In the SERS studies, gold is the most studied metal as a SERS

active substrate due to the high motion ability of the outer shell electrons which interact with SERS laser to induce an additional electromagnetic field called surface plasmon that is the main responsible for the enhanced Raman scattering [8-10]. Therefore, taking into consideration advantages of the SERS, it is a good candidate for highly sensitive, selective, and less time consuming detection method for any interested analyte such as DNA, RNA, protein, etc.

Molecular sentinel (MS) is a technique that uses a SERS active substrate and stem loop structure DNA or RNA. In this method, DNA structure is consisting of a thiol group at one end and a Raman label at the other end. DNA is immobilized on the metal surface via thiol-sulfur interaction and the Raman label molecules was located at proximity of the metal surface after immobilization. The stem loop configuration is disturbed by the complementary DNA/RNA and the Raman label is moved from the metal surface which induce the decreasing of the Raman scattering [11,12]. Thus, it is possible to correlate the concentration of the target DNA/RNA and the decreasing of the SERS intensity.

In the present study, a novel MS based SERS sensor was designed for detection of HCV DNA. For this purpose, magnetic gold nanoparticles were synthesized and then, functionalized with stem loop structure HCV DNA. After hybridization, the decreasing of Raman intensity was monitored by SERS. For all the detection steps, only one hybridization process was done and centrifugal separation and post-hybridization washing steps were omitted due to simple magnetic separation of the particles by an external magnet and monitoring only Raman label molecule, respectively. It is believed that the prepared sensor offers sensitive, selective, fast and reliable detection of HCV DNA.

MATERIALS and METHODS

All chemicals used this study were supplied from Sigma-Aldrich (Germany) and used as received unless otherwise stated. Stem-loop hairpin (MS), complementary (target) and non-complementary DNAs were purchased from Daejeon, Korea. The sequences were listed in Table 1. The underlined sequences shows the complementary arms of the stem-loop DNA, and the bold sequences indicates the complementary DNA to the loop region of the MS hairpin. Ultrapure deionized water was used in all experimental studies.

Synthesis of magnetic gold nanoparticles (Fe_3O_4@Au)

Fe_3O_4 nanoparticles were synthesized by co-precipitation method as reported previously [13]. The prepared magnetic nanoparticles were dispersed in 0.1% wt of sodium citrate solution to prevent agglomeration of the magnetic nanoparticles. 500 µL of the magnetic suspension was added to the 100 mL of deionized water and the nanoparticles were well dispersed by an ultrasonic bath at room temperature. The black suspension was heated to 80 °C and stirred with mechanical stirrer at 900 rpm for 1 hour and then, 50 µL 10 mM of $HAuCl_4$ was added to the suspension. The hot plate was removed after the color of the suspension turned to red. After cooling to room temperature, nanoparticles was collected by an external magnet and washed with deionized water for several times and re-dispersed in deionized water. The red suspension was stored at +4 °C until needed.

Preparation of MS probe (Fe_3O_4@Au@MS)

10 mg of the Fe_3O_4@Au nanoparticles were dispersed in 4 mL of 0.01 M phosphate buffer saline containing 200 µM $MgCl_2$ (PBS, pH 7.4) (for the optimization of the salt concentration, please see Supplementary Material) by ultrasonication for 10 min at room temperature and 1 mL of 1.0 µM thiolated stem-loop DNA (MS) solution (0.01M PBS, pH 7.4) was added to the particle dispersion and left to react on a shaker for 2 hours. Then, the nanoparticles was collected by a magnet and washed three times with PBS to remove physically adsorbed MS on magnetic gold nanoparticles and redispersed in 5.0 mL of PBS buffer. The unoccupied gold surface by MS probe was passivated with 2-mercaptoethanol (ME) to reduce non-specific binding of HCV DNA on the gold surface. For this purpose, 1.0 mL of 1 mM ethanolic solution of ME was added to the PBS buffer containing MS probe and left to react on a shaker for overnight. The passivated MS probe was collected by an external magnet and washed again with PBS buffer for three times and lastly redispersed in 5.0 mL of PBS buffer.

Hybridization with target HCV DNA

50 µL of the MS probe and 20 µL of the target HCV DNA sample with a concentration range 0-50 pM in 0.01 M PBS containing 200 µM $MgCl_2$ were mixed and maintained on a shaker at 37 °C. After 15 min. incubation

Table 1. DNA sequences used in the present study.

Name	*Sequence*
Stem-loop DNA (MS, capture probe)	*5′-SH-AAAAA<u>CACAUC</u>**TGCCGCGGA TATTAGGAT**<u>GTGTG</u>-R6G-3′*
Complementary DNA (target DNA or HCV DNA)	*3′-**ACG GCG CCT ATA ATC CTA** -5′*
Non-complementary DNA	*5′-TAGAGGAACGAGGTACCAGCGACG-3′*

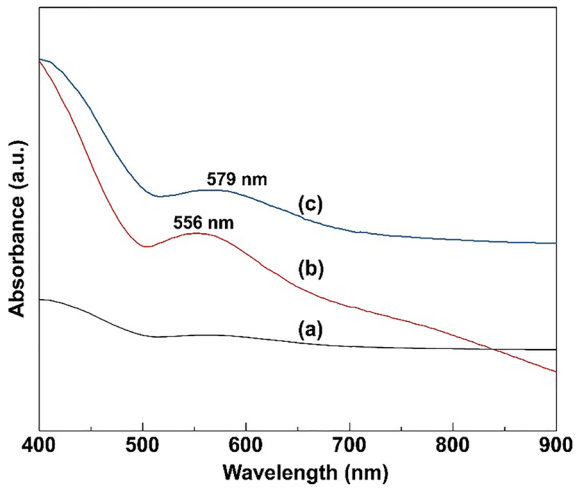

Figure 1. UV-vis spectra of (a) Fe_3O_4, (b) Fe_3O_4@Au, (c) Fe_3O_4@Au@MS

time, the magnetic nanoparticles were collected and redispersed in PBS buffer. Then, 25 µL of the dispersion was dropped on the freshly cleaned silicon surface for SERS measurements. The same protocol was applied for non-complementary DNA.

Optical properties of the prepared nanoparticles were examined by UV-vis spectrophotometer (Shimadzu UV-2550) at room temperature. The morphology and diameter of the nanoparticles were determined by transmission electron microscopy (TEM, JEOL 1400). The mean diameter of the nanoparticles was calculated by using ImageJ software. X-ray photoelectron spectroscopy (XPS) analysis was examined by a SPECS XPS spectrometer using Al Kα as a X-ray source. Magnetic properties of the nanoparticles were characterized by vibrating sample magnetometer (VSM) from Cryogenic Limited PPMS system. DeltaNu Examiner Raman microscope (DeltaNu Inc., Laramie, WY) with a 785-nm laser source was used for SERS analysis. All spectra were collected with 140-mW laser power, for 5-s acquisition time. Baseline correction was done for all spectra.

RESULTS and DISCUSSION

Characterization of Fe_3O_4@Au and Fe_3O_4@Au@MS

The optical properties of the prepared nanoparticles were investigated by UV-vis absorption spectroscopy. After coating of gold shell on the Fe_3O_4 nanoparticles, a new absorption peak at about 556 nm was obtained (Fig. 1b) that is the characteristic absorbance peak of the gold nanoparticle. After immobilization of the MS probe on gold shell, a 21 nm a red shift of the absorption wavelength from 556 nm to 579 nm as a result of the changing of the refractive index of the nanoparticle by surrounding media (Fig. 1c). Moreover, the absorption peaks for both Fe_3O_4@Au and Fe_3O_4@Au@MS were relatively narrow indicating the nanoparticles did not agglomerate in the solution [14].

The mean diameter and morphology of the nanoparticles were determined by TEM analysis and TEM images were presented in Fig. 2. The Fe_3O_4 nanoparticles (Fig. 2a) have an irregular structures with a mean diameter approximately 6.1 ± 1.8 nm (accounted on 185 nanoparticles). After the formation of gold shell on the Fe_3O_4 nanoparticles, mean diameter of the nanoparticle increased to 14.4 ± 3.1 nm (accounted on 228 nanoparticles) indicating the formation of nearly 4.0 nm gold shell on the Fe_3O_4 nanoparticles. After the formation of gold shell, the MS probe was attached on the Fe_3O_4@Au nanoparticles and the diameter of the nanoparticles increased to 20.5 ± 3.8 nm (accounted on 169 nanoparticles). The nearly 6 nm difference between Fe_3O_4@Au and Fe_3O_4@Au@MS nanoparticles was due to the presence of the 33-base DNA on the magnetic gold nanoparticles. As seen from Fig. 2, all nanoparticles were agglomerated after drying on the TEM grids. This was probably due to high magnetization properties of the nanoparticles in solid state [13].

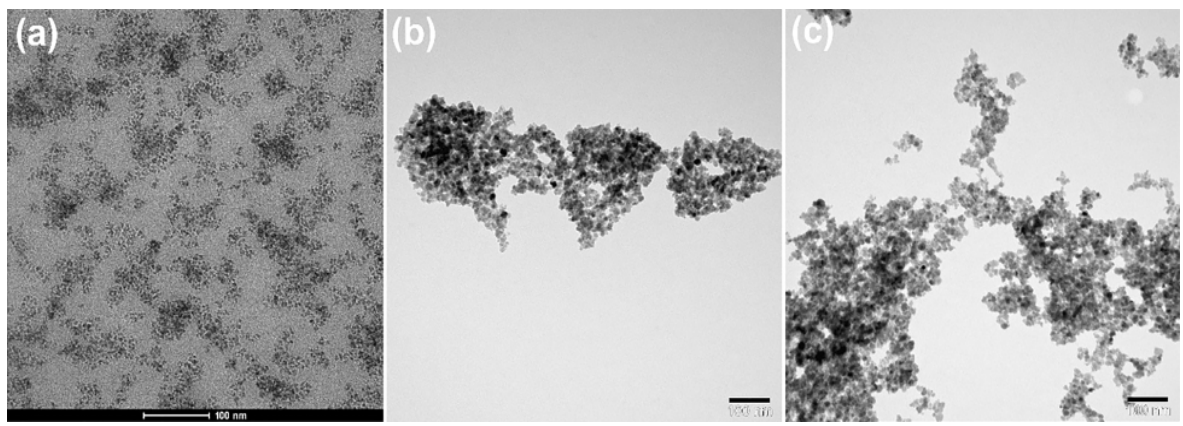

Figure 2. TEM images of (a) Fe_3O_4, (b) Fe_3O_4@Au, (c) Fe_3O_4@Au@MS.

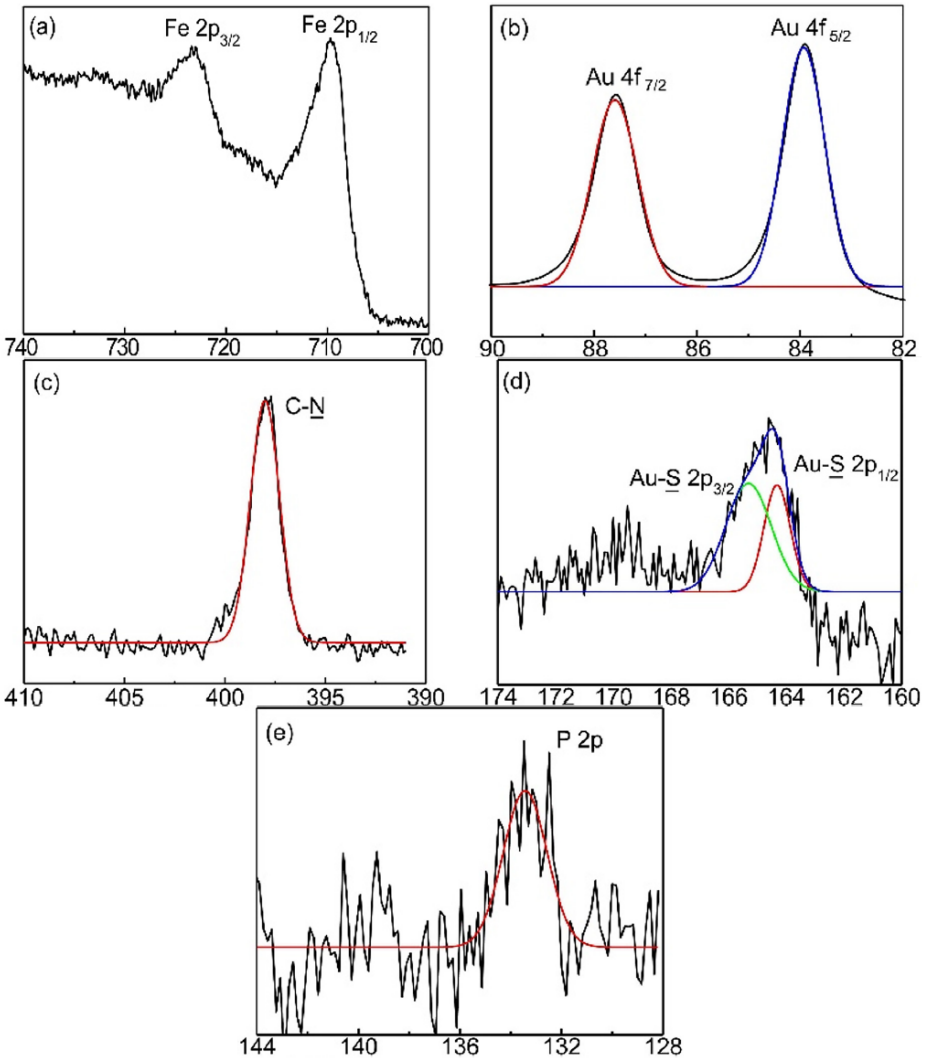

Figure 3. Core-level XPS spectra of (a) Fe2p, (b) Au4f, (c) N1s, (d) S2p, (e) P2p for Fe_3O_4@Au@MS.

Immobilization of the MS probe on the magnetic gold nanoparticles was confirmed with XPS. Core-level XPS spectra of the Fe_3O_4@Au@MS were shown in Figure 3. The core-level XPS spectrum of Fe2p was fitted to two component at about 723.1 eV and 709.5 eV belonging to $Fe2p_{3/2}$ and $Fe2p_{1/2}$, respectively (Fig. 3a). The core level XPS spectra of Au4f was fitted to two different peaks at about 87.4 eV and 83.7 eV corresponding to $Au4f_{7/2}$ and $Au4f_{5/2}$, respectively (Fig. 3b). Moreover, the core-level XPS spectra of N1s, S2p and P2p was fitted to the components with binding energies at about 398.9 eV (C-N) for N 1s (Fig. 3c), 165.0 eV (Au-S$2p_{3/2}$) and 164.2 eV (Au-S$2p_{1/2}$) for S2p (Fig. 3d) and 133.2 eV for P2p (Fig. 3e). The presence of N, P and S elements in the core-level spectra of Fe_3O_4@Au@MS strongly indicated that the covalent attachment of MS probe on the Fe_3O_4@Au nanoparticle were successful.

The saturation magnetization (M_s) values of the all nanoparticles were determined with VSM at room temperature. The magnetic hysteresis curves of the nanoparticles were presented in Figure 4. The M_s value of the Fe_3O_4 nanoparticles was found to be 62.8 emu/g (Fig. 4a). After the M_s of the Fe_3O_4 nanoparticles drastically decreased to 36.8 emu/g due to the formation of Au shell on the Fe_3O_4 nanoparticles (Fig. 4b). The covalent attachment of the MS probe on the Fe_3O_4@Au nanoparticles, the M_s value of the magnetic nanoparticles slightly decreased to 29.5 emu/g (Fig. 4c) that is the sufficient M_s value for using magnetic nanoparticles in biological applications [15,16]. Moreover, in all cases, the magnetic hysteresis curves also showed no remanence or coercivity indicating that all the prepared magnetic nanoparticles had superparamagnetic behavior at room temperature.

SERS detection of the target DNA

SERS detection of the target DNA step was shown in Fig. 5. After immobilization of the MS probe DNA on the Fe_3O_4@Au nanoparticles, the rhodamine 6G (R6G)

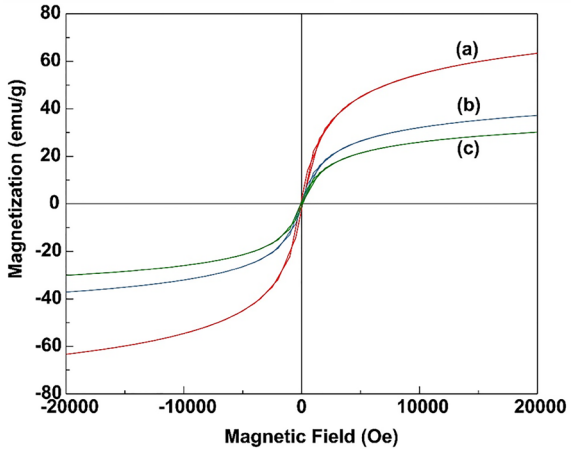

Figure 4. Magnetic hysteresis curves of (a) Fe_3O_4, (b) Fe_3O_4@Au, (c) Fe_3O_4@Au@MS nanoparticles at room temperature.

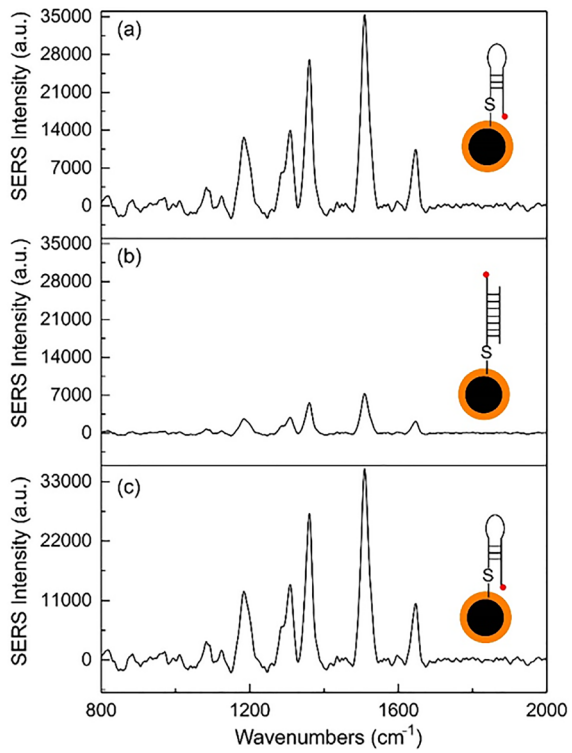

Figure 5. SERS spectrum of (a) Fe_3O_4@Au@MS (blank), (b) Fe_3O_4@Au@MS in the presence of target HCV DNA (concentration: 40 pM), (c) Fe_3O_4@Au@MS in the presence of non-complementary HCV DNA.

label on the 3´-end of the MS probe was located to the Au shell and resulted a strong SERS signal (Fig. 5a). When the complementary DNA was added to the Fe_3O_4@Au@MS nanoparticles, the hybridization took place and the stem-loop structure was opened and R6G was located far away from the Au shell and induced a decreasing SERS intensity (Fig. 5b). Moreover, in the presence of the non-complementary DNA, there was no change in the SERS intensity indicating no hybridization took place and the R6G was still remained close to the Au shell (Fig. 5c). This result also showed the selectivity of the prepared MS based SERS sensor.

It was further investigated to verify the usability of the Fe_3O_4@Au@MS nanoparticles for quantitative DNA detection for the HCV. For this purpose, the Fe_3O_4@Au@MS nanoparticles were incubated with different HCV target DNA with concentration between 0-50 pM and four different measurements were taken for per sample and averaged in a single spectrum. Fig. 6a illustrated the SERS spectra of the MS probe with different amount of target HCV DNA. The SERS intensity decreased when the target DNA concentration increased. This results also suggested that there could be a linear relationship between the decreasing of the SERS intensity and the target DNA concentration. To determine the limit of detection (LOD), the most intensive Raman peak of R6G located at 1506 cm^{-1} was selected. As shown in Fig. 6b, a linear relationship with a correlation coefficient (R^2) of 0.9986 was obtained and the LOD was found to be 0.1 pM from $3S_{blank}/m$ where S_{blank} is the standard deviation of the blank (i.e.in the absence of target HCV DNA) and m is the slope of the calibration curve. Compared with the other HCV DNA detection methods, the developed MS based SERS sensor could provide a higher sensitivity [4, 17-19]. In addition, the lower LOD shows that the prepared sensor can be a powerful diagnostic tool for the detection of HCV in the early stage of infection.

CONCLUSION

In summary, it has been demonstrated a novel SERS biosensor design for the detection of HCV. The MS based sensor is relatively easy to prepare, low-cost and could detect the complementary DNA with high selectivity. The prepared sensor has magnetic property which allows the separation of the nanoparticles easily by an external magnet without any centrifuge step. In addition, the sensor does not need labelling the target DNA, and post-hybridization washing steps. The prepared sensor

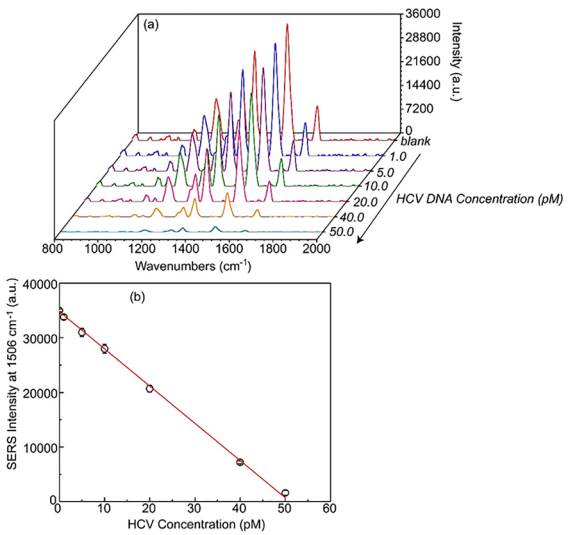

Figure 6. (a) SERS spectra of Fe_3O_4@Au@MS after hybridization with different amount of HCV DNA, (b) SERS intensity changing as a function of HCV DNA concentration.

can be extended to point-of-care disease with the help of commercially available portable, hand-held Raman spectroscopy.

ACKNOWLEDGEMENTS

The author thanks to Prof. Dr. Zekiye Suludere for TEM analysis and also thanks to Prof. Dr. Uğur Tamer for his valuable contributions for SERS measurements.

REFERENCES

1. Guillou–Guillemette HL and Lunel–Fabiani F, Detection and quantification of serum or plasma HCV RNA: Mini review of commercially available assays, in hepatitis C: Methods and protocols. ed. H. Tang, Humana Press, Totowa, NJ, 2nd edn 150 (2009) 3-14.
2. Zobair MY, Hepatitis C infection: A systemic disease, Clinics in Liver Disease 21 (2017) 449–453.
3. Thomas JR and Hergenrother PJ, targeting RNA with small molecules. Chemical Reviews 108 (2008) 1171–1224.
4. Li W, Wu P, Zhang H and Cai C, Catalytic signal amplification of gold nanoparticles combining with conformation–switched hairpin DNA probe for hepatitis C virus quantification. Chemical Communications 48 (2008) 7877-7879.
5. Liu L, Wang X, Ma Q, Lin Z, Chen S, [Li Y,] Lu L, [Qu] H and Su X, Multiplex electrochemiluminescence DNA sensor for determination of hepatitis B virus and hepatitis C virus based on multicolor quantum dots and Au nanoparticles. Analytica Chimica Acta 916 (2016) 92–101.
6. Skladal P, Riccardi CS, Yamanaka H and Costa PI, Piezoelectric biosensors for real–time monitoring of hybridization and detection of hepatitis C virus. Journal of Virological Methods 117 (2004) 145–151.
7. Wenbing L, Xinchu Z, Zhifeng Y, Glushenkov AM, and Kong L, Plasmonic substrates for surface enhanced Raman scattering. Analytica Chimica Acta 984 (2017) 19–41.
8. Cho I–H, Das M, Bhandari P, and Irudayaraj J, High performance immunochromatographic assay combined with surface enhanced Raman spectroscopy. Sensors and Actuators B: Chemical, 213 (2015) 209–214.
9. Herrera G, Padilla A, and Rivera SH, Surface enhanced Raman scattering (SERS) studies of gold and silver nanoparticles prepared by laser ablation. Nanomaterials 3 (2013) 158–172.
10. Stockman MI, Nanoplasmonics: past, present, and glimpse into future. Optics Express 19 (2011) 22029–22106.
11. Pang Y, Wang J, Xiao R, Wang S, SERS molecular sentinel for the RNA genetic marker of PB1–F2 protein in highly pathogenic avian influenza (HPAI) virus. Biosensors and Bioelectronics 61 (2014) 460–465.
12. Wang H–N, Fales AM, Zaas AK, Woods CW, Burke T, Ginsburg GS, Vo–Dinh T, Surface–enhanced Raman scattering molecular sentinel nanoprobes for viral infection diagnostics. Analytica Chimica Acta 786 (2013) 153–158.
13. Tumturk H, Sahin F and Turan E, Magnetic nanoparticles coated with different shells for bio recognition high specific binding capacity. Analyst 139 (2014) 1093-1100.
14. Haiss W, Thanh NTK, Aveyard J, and Fernig DG, Determination of size and concentration of gold nanoparticles from UV÷Vis spectra. Analytical Chemistry 79 (2007) 4215-4221.
15. Qin W, Song Z, Fan C, Zhang W, Cai Y, Zhang Y, and Qian X, Trypsin immobilization on hairy polymer chains hybrid magnetic nanoparticles for ultrafast, highly efficient proteome digestion, facile ^{18}O labeling and absolute protein quantification. Analytical Chemistry 84 (2012) 3138-3144.
16. Kouassi GK, and Irudayaraj J, Magnetic and gold–coated magnetic nanoparticles as a DNA sensor. Analytical Chemistry 78 (2006) 3234-3241.
17. Griffin J, Singh AK, Senapati, Lee E, Gaylor K, Jones–Boone J. and Ray PC, Sequence–specific HCV RNA quantification using the size–dependent nonlinear optical properties of gold nanoparticles. Small 5 (2009) 5, 839.
18. Liu S, Hu Y, Jin J, Zhang H and Cai CX, Electrochemical detection of hepatitis C virus based on site–specific DNA cleavage of BamHI endonuclease. Chemical Communications 2009, 1635–1637.
19. Liu S, Wang Q, Chen D, Jin J, Hu Y, Wu P, Zhang H and Cai CX, Electrochemical approach for the specific detection of hepatitis C virus based on site–specific DNA cleavage of BamHI endonuclease. Analytical Methods 2 (2010) 135–142.